Photoproduction in Ultra-Peripheral Relativistic Heavy Ion Collisions at STAR

Boris Grube

Excellence Cluster Universe
Technische Universität München, Garching, Germany

for the STAR Collaboration

13th International Conference on Elastic & Diffractive Scattering
CERN, Geneva, 2nd July 2009

Outline

1. Introduction
   - Ultra-peripheral relativistic heavy ion collisions
   - Experimental setup
   - Triggering and data selection

2. Results on photonuclear vector meson production in Au $\times$ Au collisions
   - ρ photoproduction cross section
   - Interference effects in ρ photoproduction
   - $\pi^+\pi^-\pi^+\pi^-$ photoproduction

Outline

1. Introduction
   - Ultra-peripheral relativistic heavy ion collisions
   - Experimental setup
   - Triggering and data selection
2. Results on photonuclear vector meson production in Au $\times$ Au collisions
   - ρ photoproduction cross section
   - Interference effects in ρ photoproduction
   - $\pi^+\pi^-\pi^+\pi^-$ photoproduction

Ultra-Peripheral Heavy Ion Collisions (UPC)

- Nuclei surrounded by cloud of quasi-real virtual photons
- Number of photons large ($\propto Z^2$)
- Fast-moving heavy ions produce intense photon flux
  - Described by Weizsäcker-Williams approximation ("nuclear flashlight")
- Nuclear collisions: long range interaction via electromagnetic fields in addition to hadronic interactions
- Require $b > R_A + R_B$ to exclude (otherwise inseparable) hadronic interactions

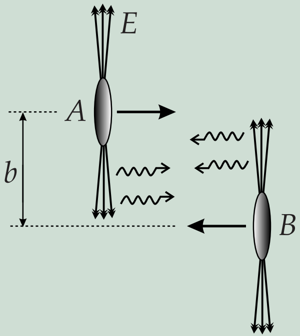

Photonuclear interactions in UPCs

Vector meson production

1. **Exclusive production**
   - γ^* from "emitter" nucleus fluctuates into $q\bar{q}$-pair
   - $q\bar{q}$-pair scatters off "target" nucleus into real vector meson
   - Scattering described in terms of soft Pomeron exchange

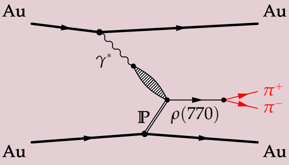

2. **Production accompanied by mutual nuclear breakup**
   - Predominantly Coulomb excitation of Giant Dipole Resonances (GDRs)
   - Independent of meson production
   - GDRs decay via neutron emission
     $\Longrightarrow$ distinctive signature

Photonuclear interactions in UPCs

Vector meson production

1. **Exclusive production**
   - γ^* from "emitter" nucleus fluctuates into $q\bar{q}$-pair
   - $q\bar{q}$-pair scatters off "target" nucleus into real vector meson
   - Scattering described in terms of soft Pomeron exchange

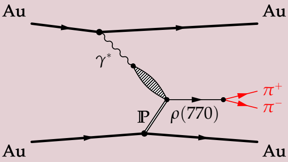

2. **Production accompanied by mutual nuclear breakup**
   - Predominantly Coulomb excitation of Giant Dipole Resonances (GDRs)
   - Independent of meson production
   - GDRs decay via neutron emission $\Longrightarrow$ distinctive signature

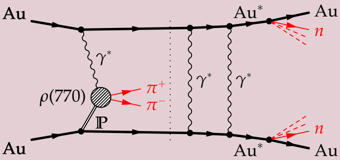

The STAR Experiment at RHIC

Detector components important for UPC measurements

NIM **A499**

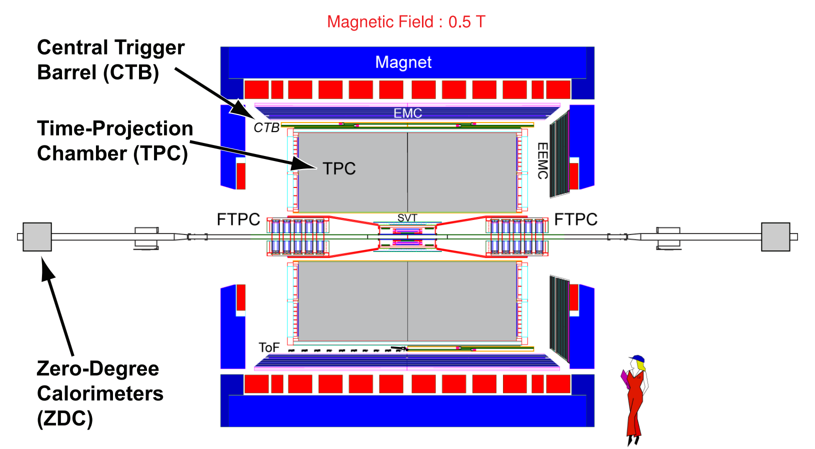

Triggering and Data Selection

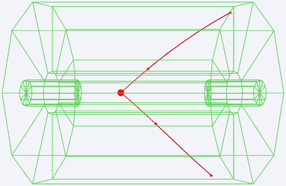

Clean 2-prong event

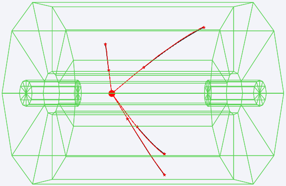

Clean 4-prong event

Experimental signature and event selection

- Low overall track multiplicity
- 2 or 4 well reconstructed tracks
  - From common vertex
  - Zero net charge
- Vertex position close to interaction diamond
- Coherent production dominates: produced vector mesons have low $p_T \lesssim 2\hbar/R_A \approx 60$ MeV/c
- For nuclear breakup: additional forward neutrons $\Longrightarrow$ trigger

STAR acceptance limits accessible rapidities to $|y| < 1$

Triggering and Data Selection

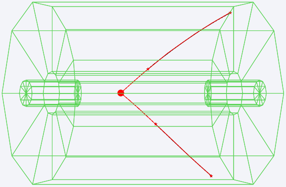

Clean 2-prong event

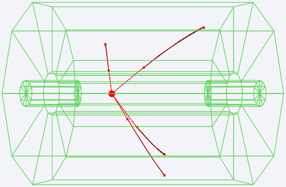

Clean 4-prong event

Experimental signature and event selection

- Low overall track multiplicity
- 2 or 4 well reconstructed tracks
  - From common vertex
  - Zero net charge
- Vertex position close to interaction diamond
- Coherent production dominates: produced vector mesons have low $p_T \lesssim 2\hbar / R_A \approx 60\ \mathrm{MeV}/c$
- For nuclear breakup: additional forward neutrons $\Longrightarrow$ trigger

STAR acceptance limits accessible rapidities to $|y| < 1$

Triggering and Data Selection

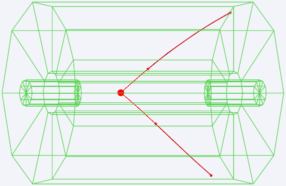

Clean 2-prong event

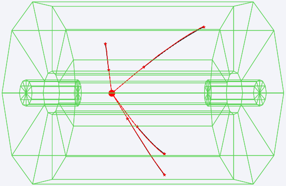

Clean 4-prong event

Experimental signature and event selection

- Low overall track multiplicity
- 2 or 4 well reconstructed tracks
  - From common vertex
  - Zero net charge
- Vertex position close to interaction diamond
- Coherent production dominates: produced vector mesons have low $p_T \lesssim 2\hbar / R_A \approx 60$ MeV/c
- For nuclear breakup: additional forward neutrons $\Longrightarrow$ trigger

STAR acceptance limits accessible rapidities to $|y| < 1$

Triggering and Data Selection

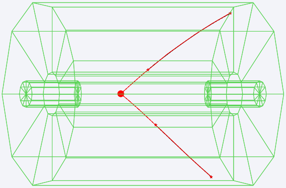

Clean 2-prong event

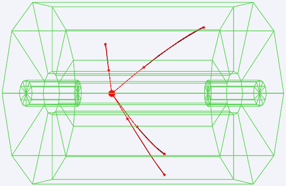

Clean 4-prong event

Experimental signature and event selection

- Low overall track multiplicity
- 2 or 4 well reconstructed tracks
  - From common vertex
  - Zero net charge
- Vertex position close to interaction diamond
- Coherent production dominates: produced vector mesons have low $p_T \lesssim 2\hbar / R_A \approx 60$ MeV/c
- For nuclear breakup: additional forward neutrons $\Longrightarrow$ trigger

STAR acceptance limits accessible rapidities to $|y| < 1$

UPC Triggers

2 triggers used at STAR

1. **Topology trigger** (CTB only)
   - CTB is subdivided into 4 quadrants
   - Top+Bottom quadrants veto cosmic rays
   - Coincidence of North and South quadrants
   - **Does not require nuclear breakup**

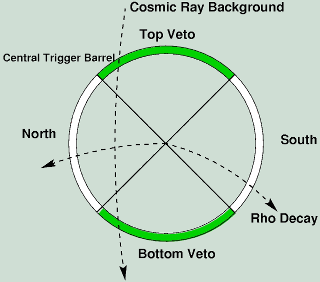

2. **Minimum bias trigger** (CTB + ZDC)
   - Low hit multiplicity in CTB
   - Coincident neutrons from nuclear breakup in both ZDCs

PR **C77**, 034910 (2008)

UPC Triggers

2 triggers used at STAR

1. **Topology trigger** (CTB only)
   - CTB is subdivided into 4 quadrants
   - Top+Bottom quadrants veto cosmic rays
   - Coincidence of North and South quadrants
   - **Does not require nuclear breakup**

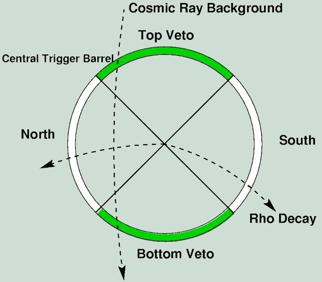

2. **Minimum bias trigger** (CTB + ZDC)
   - Low hit multiplicity in CTB
   - Coincident neutrons from nuclear breakup in both ZDCs

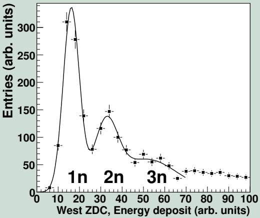

PR **C77**, 034910 (2008)

Outline

1. Introduction
   - Ultra-peripheral relativistic heavy ion collisions
   - Experimental setup
   - Triggering and data selection

2. Results on photonuclear vector meson production in Au $\times$ Au collisions
   - ρ photoproduction cross section
   - Interference effects in ρ photoproduction
   - $\pi^+\pi^-\pi^+\pi^-$ photoproduction

ρ Production in Au × Au @ $\sqrt{s_{NN}} = 200$ GeV

PR **C77**, 034910 (2008)

$\pi^+\pi^-$ invariant mass distributions (acceptance corrected)

1. **Topology trigger**
   - No nuclear breakup required

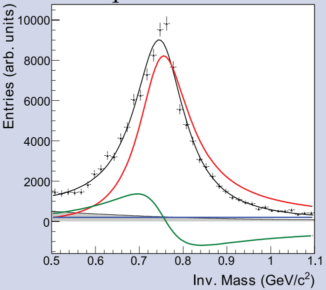

2. **Minimum bias trigger**
   - ZDC neutron tag

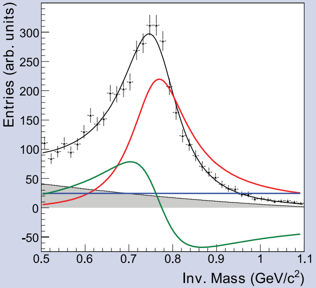

- Background estimate (gray shaded) from like-sign pairs $\pi^\pm\pi^\pm$
- Mass spectrum fit with relativistic p-wave Breit-Wigner with Söding interference term (direct $\pi^+\pi^-$ production)

ρ Production Cross Section

Comparison with model predictions for Au $\times$ Au @ $\sqrt{s_{NN}} = 200$ GeV

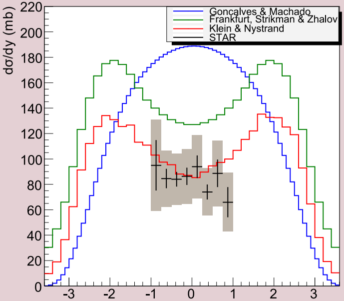

PR **C77**, 034910 (2008)

1. **Klein, Nystrand** PR **C60**, 014903 (1999)
   - Vector Dominance Model (VDM) for $\gamma^* \longrightarrow |q\bar{q}\rangle$
   - Classical mechanical approach for scattering
   - Uses photoproduction data from $\gamma p \rightarrow \rho p$ experiments
2. **Frankfurt, Strikman, Zhalov** PR **C67**, 034901 (2003)
   - generalized VDM
   - QCD Gribov-Glauber approach
3. **Gonçalves, Machado** EPJ **C29**, 271-275 (2003)
   - QCD color dipole approach
   - Includes nuclear effects and parton saturation phenomena

- Limited y-range does not allow to discriminate shapes
- Klein, Nystrand model agrees well with data

ρ Production Cross Section

Energy dependence

- STAR measured ρ production cross section (total and with mutual nuclear breakup)
  1. At $\sqrt{s_{NN}} = 130\,\text{GeV}$ PRL **89**, 272302 (2002)
  2. At $\sqrt{s_{NN}} = 200\,\text{GeV}$ PR **C77**, 034910 (2008)
  3. Ongoing analysis for $\sqrt{s_{NN}} = 62\,\text{GeV}$

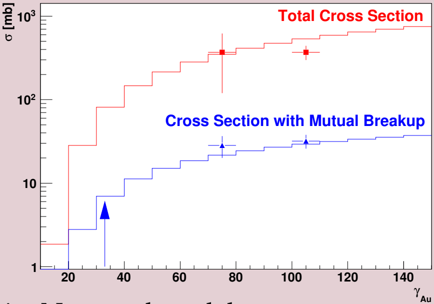

- Solid line: Klein, Nystrand model PR **C60**, 014903 (1999)

Interference Effects in ρ Photoproduction

PRL **102**, 112301 (2009)

Two-source interferometer

- Cannot distinguish γ^* source and target
- ρ production occurs close to target nucleus ($d \lesssim 1\,\text{fm}$)

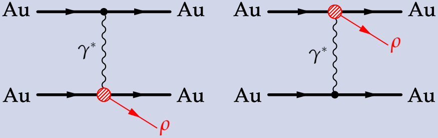

- Two indistinguishable processes related by parity transformation
- $\mathbb{P}(\rho) = -1 \implies$ subtract amplitudes
  $$\sigma = \left| A(p_T, b, y) - A(p_T, b, -y)\, e^{i\vec{p}_T\cdot\vec{b}} \right|^2$$
- At midrapidity $A(p_T, b, y) \approx A(p_T, b, -y)$
  $$\implies \sigma(p_T, b, 0) = 2\,|A(p_T, b, 0)|^2 \left[1 - \cos(\vec{p}_T \cdot \vec{b})\right]$$
- System acts like two-slit interferometer with slit separation $|\vec{b}|$

Interference Effects in ρ Photoproduction

PRL **102**, 112301 (2009)

Two-source interferometer

- ρ production suppressed for $p_T \lesssim \hbar/\langle b\rangle$
- $t(\approx p_T^2)$-Spectrum roughly exponential with significant downturn for $t < 0.0015\,\mathrm{GeV}^2$
  - Consistent with Monte-Carlo including interference effect

Raw minimum bias t-spectrum for $|y| \in [0, 0.5]$

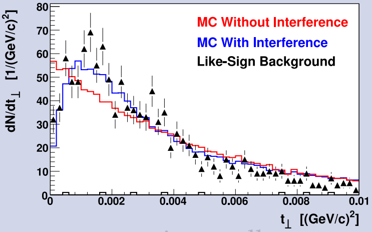

- Since $\beta\gamma c\tau \ll \langle b\rangle$, produced ρ decay at two points well separated in space-time
  - Two amplitudes overlap and interfere only after decay
  - Interference must involve $\pi^+\pi^-$ final state
  - Interference only possible for entangled nonlocal final state wave function that is not factorizable into separate $\pi^\pm$ wave functions
  - Example of Einstein-Podolsky-Rosen paradox with continuous variables momentum and position

Interference Effects in ρ Photoproduction

PRL **102**, 112301 (2009)

Two-source interferometer

- ρ production suppressed for $p_T \lesssim \hbar/\langle b\rangle$
- $t(\approx p_T^2)$-Spectrum roughly exponential with significant downturn for $t < 0.0015\,\mathrm{GeV}^2$
  - Consistent with Monte-Carlo including interference effect

Raw minimum bias t-spectrum for $|y| \in [0, 0.5]$

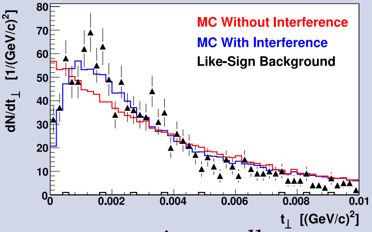

- Since $\beta\gamma c\tau \ll \langle b\rangle$, produced ρ decay at two points well separated in space-time
  - Two amplitudes overlap and interfere only after decay
  - Interference must involve $\pi^+\pi^-$ final state
  - Interference only possible for entangled nonlocal final state wave function that is not factorizable into separate $\pi^\pm$ wave functions
  - Example of Einstein-Podolsky-Rosen paradox with continuous variables momentum and position

Interference Effects in ρ Photoproduction

PRL **102**, 112301 (2009)

Measuring interference strength

- Fit t-spectrum with $\frac{\mathrm{d}N}{\mathrm{d}t} = a\,e^{-kt}\,[1 + c\,(R(t) - 1)]$
  - k is slope parameter
  - Ratio $R(t) \equiv \frac{\text{MC } t\text{-spectrum with interference}}{\text{MC } t\text{-spectrum without interference}}$
  - Fit parameter c measures strength of interference
    - $c = 0$ corresponds to no interference
    - $c = 1$ interference predicted by Klein-Nystrand model PRL **84**, 2330 (2000)
- Different median impact parameters $\tilde{b}$
  - Topology data (no neutron tag): $\tilde{b} \approx 46\,\mathrm{fm}$
  - Minimum bias data (neutron tag): $\tilde{b} \approx 18\,\mathrm{fm}$

  $\Longrightarrow$ interference effects extend to larger p_T
- Dependence of ρ production amplitudes on photon energy decreases interference effect at larger rapidities

Measured spectral modification parameter

$$c = 87 \pm 5_{\text{stat.}} \pm 8_{\text{syst.}}\ \%$$

Interference Effects in ρ Photoproduction

PRL **102**, 112301 (2009)

Measuring interference strength

- Fit t-spectrum with $\frac{dN}{dt} = a\, e^{-kt}\left[1 + c\,(R(t) - 1)\right]$
  - k is slope parameter
  - Ratio $R(t) \equiv \frac{\text{MC } t\text{-spectrum with interference}}{\text{MC } t\text{-spectrum without interference}}$
  - Fit parameter c measures strength of interference
    - $c = 0$ corresponds to no interference
    - $c = 1$ interference predicted by Klein-Nystrand model PRL **84**, 2330 (2000)
- Different median impact parameters $\tilde{b}$
  - Topology data (no neutron tag): $\tilde{b} \approx 46\,\mathrm{fm}$
  - Minimum bias data (neutron tag): $\tilde{b} \approx 18\,\mathrm{fm}$

  $\Longrightarrow$ interference effects extend to larger p_T
- Dependence of ρ production amplitudes on photon energy decreases interference effect at larger rapidities

Measured spectral modification parameter

$$c = 87 \pm 5_{\text{stat.}} \pm 8_{\text{syst.}}\ \%$$

$\pi^+\pi^-\pi^+\pi^-$ Production in Au $\times$ Au @ $\sqrt{s_{NN}} = 200\,\text{GeV}$

Coherent photonuclear production with mutual nuclear excitation

- Enhancement at low p_T due to coherent production

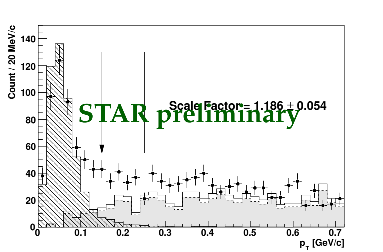

- Mass peak could be $\rho(1450)$ and/or $\rho(1700)$
  - Similar to peak seen in γp experiments
- Fit with s-wave Breit-Wigner modified by Ross-Stodolsky factor
  - $f(m) = A \cdot \left(\frac{m_0}{m}\right)^n \cdot \frac{m_0^2\Gamma_0^2}{(m_0^2 - m^2)^2 + m_0^2\Gamma_0^2} + f_{BG}(m)$
  - $m_0 = 1540 \pm 40$ MeV/c^2, $\Gamma_0 = 570 \pm 60$ MeV

$\pi^+\pi^-\pi^+\pi^-$ Production in Au $\times$ Au @ $\sqrt{s_{NN}} = 200\,\text{GeV}$

Coherent photonuclear production with mutual nuclear excitation

- Enhancement at low p_T due to coherent production

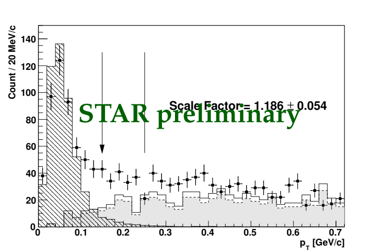

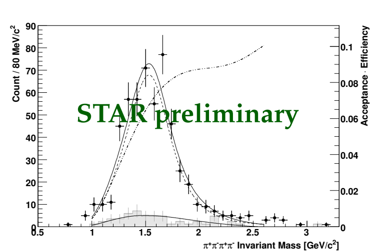

- Mass peak could be $\rho(1450)$ and/or $\rho(1700)$
  - Similar to peak seen in γp experiments
- Fit with s-wave Breit-Wigner modified by Ross-Stodolsky factor
  - $f(m) = A \cdot \left(\frac{m_0}{m}\right)^n \cdot \frac{m_0^2\Gamma_0^2}{(m_0^2 - m^2)^2 + m_0^2\Gamma_0^2} + f_{BG}(m)$
  - $m_0 = 1540 \pm 40\ \text{MeV}/c^2, \Gamma_0 = 570 \pm 60\,\text{MeV}$

$\pi^+\pi^-\pi^+\pi^-$ Production in Au $\times$ Au @ $\sqrt{s_{NN}} = 200\,\text{GeV}$

- Cross section ratio $\frac{\sigma^{\text{coh}}_{xn\,xn}[\pi^+\pi^-\pi^+\pi^-]}{\sigma^{\text{coh}}_{xn\,xn}[\rho^0(770)]} = 13.4 \pm 0.8\ \%$
- Substructure: low mass pion pair accompanied by $\rho^0(770)$
  - Decay model in MC: $\rho' \to [\rho^0(770) + f_0(600)]_{s\text{-wave}}$
- No signal seen in $\pi^+\pi^-$ channel
- Publication in preparation

$\pi^+\pi^-\pi^+\pi^-$ Production in Au $\times$ Au @ $\sqrt{s_{NN}} = 200\,\text{GeV}$

- Cross section ratio $\dfrac{\sigma^{\text{coh}}_{xn\,xn}[\pi^+\pi^-\pi^+\pi^-]}{\sigma^{\text{coh}}_{xn\,xn}[\rho^0(770)]} = 13.4 \pm 0.8\ \%$
- Substructure: low mass pion pair accompanied by $\rho^0(770)$
  - Decay model in MC: $\rho' \rightarrow [\rho^0(770) + f_0(600)]_{s\text{-wave}}$

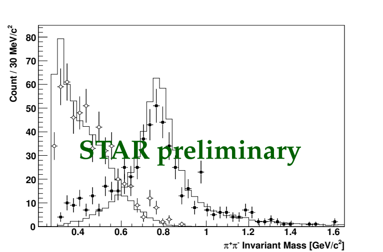

- No signal seen in $\pi^+\pi^-$ channel
- Publication in preparation

$\pi^+\pi^-\pi^+\pi^-$ Production in Au × Au @ $\sqrt{s_{NN}} = 200$ GeV

- Cross section ratio $\frac{\sigma^{\text{coh}}_{xn\,xn}[\pi^+\pi^-\pi^+\pi^-]}{\sigma^{\text{coh}}_{xn\,xn}[\rho^0(770)]} = 13.4 \pm 0.8\ \%$
- Substructure: low mass pion pair accompanied by $\rho^0(770)$
  - Decay model in MC: $\rho' \rightarrow [\rho^0(770) + f_0(600)]_{s\text{-wave}}$

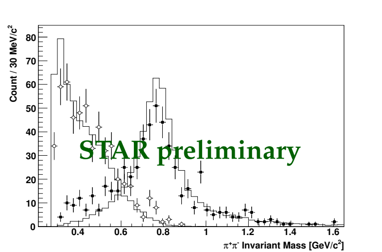

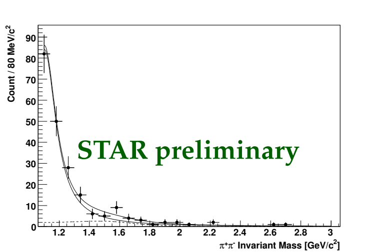

- No signal seen in $\pi^+\pi^-$ channel
- Publication in preparation

Conclusions

Summary

- STAR measured photonuclear ρ production in UPCs
  - Cross sections agree with theoretical models
  - STAR sees interference effects in ρ production close to expected level PRL **102**, 113201 (2009)
- **Ongoing analyses:**
  - ρ production in d $\times$ Au @ $\sqrt{s_{NN}} = 200\,\mathrm{GeV}$ and Au $\times$ Au @ $\sqrt{s_{NN}} = 62\,\mathrm{GeV}$
  - Resonant $\pi^+\pi^-\pi^+\pi^-$ production in Au $\times$ Au @ $\sqrt{s_{NN}} = 200\,\mathrm{GeV}$

Outlook

- New STAR subsystems being commissioned right now:
  - Replacement of CTB by time-of-flight detector
    - Better trigger performance and improved particle ID
  - Data acquisition upgrade
    - TPC can be read out with $\mathcal{O}(1\,\mathrm{kHz})$ at low dead-time

Conclusions

Summary

- STAR measured photonuclear ρ production in UPCs
  - Cross sections agree with theoretical models
  - STAR sees interference effects in ρ production close to expected level PRL **102**, 113201 (2009)
- **Ongoing analyses:**
  - ρ production in d $\times$ Au @ $\sqrt{s_{NN}} = 200\,\text{GeV}$ and Au $\times$ Au @ $\sqrt{s_{NN}} = 62\,\text{GeV}$
  - Resonant $\pi^+\pi^-\pi^+\pi^-$ production in Au $\times$ Au @ $\sqrt{s_{NN}} = 200\,\text{GeV}$

Outlook

- New STAR subsystems being commissioned right now:
  - Replacement of CTB by time-of-flight detector
    - Better trigger performance and improved particle ID
  - Data acquisition upgrade
    - TPC can be read out with $\mathcal{O}(1\,\text{kHz})$ at low dead-time

Outline

Ultra-Peripheral Relativistic Heavy Ion Collisions (UPC)

Three basic interaction processes

1. Photon-photon interactions

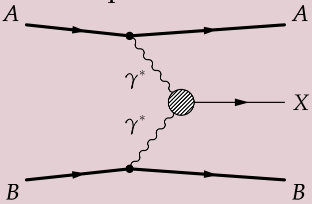

2. Photonuclear interactions

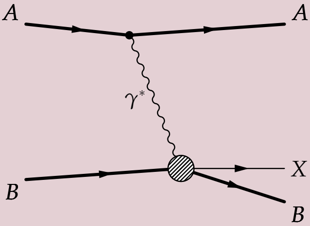

3. Nuclear breakup

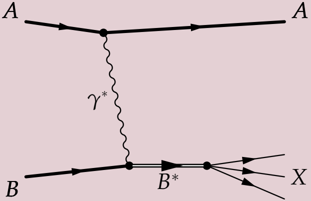

Ultra-Peripheral Relativistic Heavy Ion Collisions (UPC)

UPC kinematics for RHIC Au $\times$ Au @ $\sqrt{s_{NN}} = 200$ GeV and LHC Pb $\times$ Pb @ $\sqrt{s_{NN}} = 5500$ GeV

- Photons emitted coherently by whole nucleus
- Maximum photon energy in lab frame: $\omega_{\max} = \gamma_L \hbar c / R_A$
  $\omega_{\max} \approx 3\,\text{GeV}\ (\text{RHIC}), 80\,\text{GeV}\ (\text{LHC})$
- Photon-photon collisions: $\sqrt{s_{\gamma\gamma}^{\max}} = 2\gamma_L \hbar c / R_A$
  $\sqrt{s_{\gamma\gamma}^{\max}} \approx 6\,\text{GeV}\ (\text{RHIC}), 160\,\text{GeV}\ (\text{LHC})$
- Photonuclear interactions: $\sqrt{s_{\gamma N}^{\max}} = \sqrt{2\omega_{\max}\sqrt{s_{NN}}}$
  $\sqrt{s_{\gamma N}^{\max}} \approx 35\,\text{GeV}\ (\text{RHIC}), 950\,\text{GeV}\ (\text{LHC})$

The Relativistic Heavy Ion Collider (RHIC) at BNL

Various particle species and collision energies

- Au + Au
  - $\sqrt{s_{NN}} = 19.6, 62.4, 130$, and 200 GeV
- Cu + Cu
  - $\sqrt{s_{NN}} = 62.4$ and 200 GeV
- d + Au
  - $\sqrt{s_{NN}} = 200$ GeV
- polarized $p + p$
  - $\sqrt{s_{NN}} = 200$ and (future) 500 GeV

The STAR Experiment at RHIC

Solenoidal Tracker At RHIC (STAR)

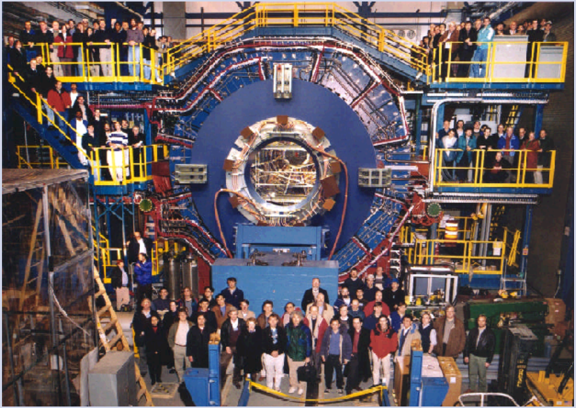

Big collaboration

- 533 scientists
- 52 institutes
- 12 countries

The STAR Experiment at RHIC

Trigger detectors

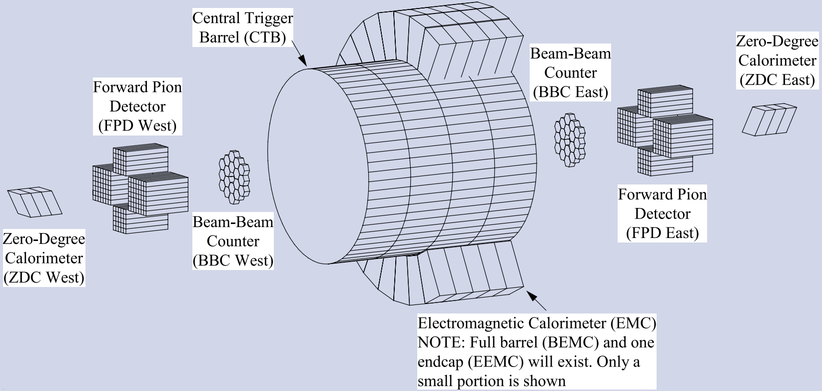

UPC Triggers — Neutron tagging

Measuring nuclear breakup neutrons in Zero Degree Calorimeter (ZDC)

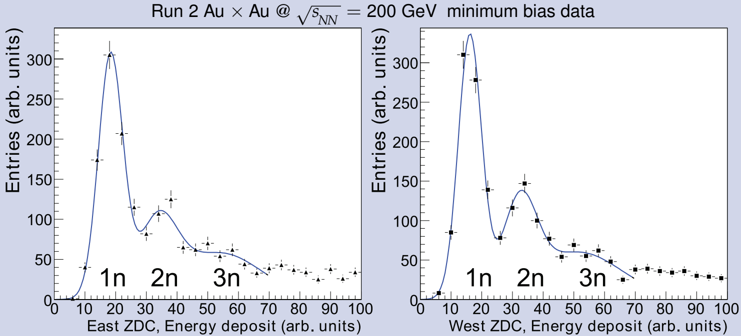

- ZDC acceptance for emitted neutrons close to 1
- Resolution good enough to see $1n, 2n, \ldots$ neutron peaks
  - Allows to select different excited states
- Neutron tag selects smaller impact parameters

UPC Triggers

Other triggers used at STAR

1. **Multi-prong trigger** (CTB and ZDC)
   - Coincident neutrons in both ZDCs
   - Low CTB multiplicity
   - Veto from large-tile BBCs
2. ***J/ψ*** **trigger** (CTB, ZDC, and BEMC)
   - Multi-prong trigger with additional calorimeter requirement
   - BEMC subdivided into 6 sectors
   - 2 high towers in non-neighboring BEMC sectors required

Triggering and Data Selection

Main background contributions

1. **Beam-gas interactions** reduced by
   - Requiring low track multiplicity
   - Limiting primary vertex position
2. **Peripheral hadronic interactions** reduced by
   - Requiring low track multiplicity
   - Selecting low p_T
3. **Pile-up events** reduced by
   - Requiring low track multiplicity
   - Limiting primary vertex position
4. **Cosmic rays** reduced by
   - Limiting primary vertex position
   - Minimum bias trigger: ZDC neutron tag
   - Topology trigger: excluding events close to $|y| = 0$

Triggering and Data Selection

Main background contributions

1. **Beam-gas interactions** reduced by
   - Requiring low track multiplicity
   - Limiting primary vertex position
2. **Peripheral hadronic interactions** reduced by
   - Requiring low track multiplicity
   - Selecting low p_T
3. **Pile-up events** reduced by
   - Requiring low track multiplicity
   - Limiting primary vertex position
4. **Cosmic rays** reduced by
   - Limiting primary vertex position
   - Minimum bias trigger: ZDC neutron tag
   - Topology trigger: excluding events close to $|y| = 0$

Triggering and Data Selection

Main background contributions

1. **Beam-gas interactions** reduced by
   - Requiring low track multiplicity
   - Limiting primary vertex position
2. **Peripheral hadronic interactions** reduced by
   - Requiring low track multiplicity
   - Selecting low p_T
3. **Pile-up events** reduced by
   - Requiring low track multiplicity
   - Limiting primary vertex position
4. **Cosmic rays** reduced by
   - Limiting primary vertex position
   - Minimum bias trigger: ZDC neutron tag
   - Topology trigger: excluding events close to $|y| = 0$

Triggering and Data Selection

Main background contributions

1. **Beam-gas interactions** reduced by
   - Requiring low track multiplicity
   - Limiting primary vertex position
2. **Peripheral hadronic interactions** reduced by
   - Requiring low track multiplicity
   - Selecting low p_T
3. **Pile-up events** reduced by
   - Requiring low track multiplicity
   - Limiting primary vertex position
4. **Cosmic rays** reduced by
   - Limiting primary vertex position
   - Minimum bias trigger: ZDC neutron tag
   - Topology trigger: excluding events close to $|y| = 0$

Triggering and Data Selection

Main background contributions

1. **Beam-gas interactions** reduced by
    - Requiring low track multiplicity
    - Limiting primary vertex position
2. **Peripheral hadronic interactions** reduced by
    - Requiring low track multiplicity
    - Selecting low p_T
3. **Pile-up events** reduced by
    - Requiring low track multiplicity
    - Limiting primary vertex position
4. **Cosmic rays** reduced by
    - Limiting primary vertex position
    - Minimum bias trigger: ZDC neutron tag
    - Topology trigger: excluding events close to $|y| = 0$

ρ Production Cross Section

Run 1 Au $\times$ Au @ $\sqrt{s_{NN}} = 130$ GeV data

p_T^{ρ} spectrum (Min. Bias)

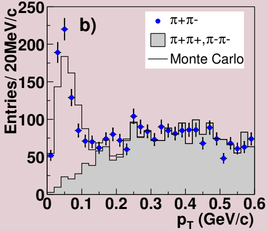

Rapidity distribution (Min. Bias)

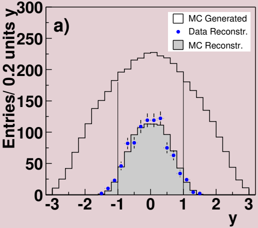

$d\sigma / dM_{\pi\pi}$ (Min. Bias)

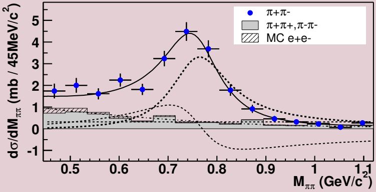

- Total cross section: $\sigma_{\text{tot}} = (460 \pm 220_{\text{stat.}} \pm 110_{\text{sys.}})$ mb

  PRL **89**, 272302 (2002)
- Theoretical prediction: $\sigma_{\text{tot}} = 350$ mb

  S. Klein *et al.*, PR **C60**, 014903 (1999)

ρ Invariant Mass Fit

PR **C77**, 034910 (2008)

Fit function with 4 components

$$\frac{d\sigma}{dM_{\pi\pi}} = \left| A \frac{\sqrt{M_{\pi\pi} M_\rho \Gamma}}{M_{\pi\pi}^2 - M_\rho^2 + i M_\rho \Gamma} + B \right|^2 + f_{BG}$$

$$\text{with } \Gamma(M_{\pi\pi}) \equiv \Gamma_\rho \frac{M_\rho}{M_{\pi\pi}} \left[\frac{M_{\pi\pi}^2 - 4m_\pi^2}{M_\rho^2 - 4m_\pi^2} \right]^{\frac{3}{2}}$$

1. Relativistic Breit-Wigner function for ρ peak with amplitude A
2. Constant direct $\pi^+\pi^-$ production amplitude B
3. Söding term for interference of the two
4. 2nd order polynomial f_{BG} describes background from like-sign pairs

Minimum bias data

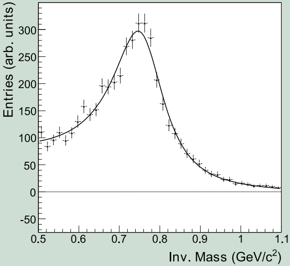

ρ Invariant Mass Fit

PR **C77**, 034910 (2008)

Fit function with 4 components

$$\frac{d\sigma}{dM_{\pi\pi}} = \left| A \frac{\sqrt{M_{\pi\pi} M_\rho \Gamma}}{M_{\pi\pi}^2 - M_\rho^2 + i M_\rho \Gamma} + B \right|^2 + f_{BG}$$

$$\text{with } \Gamma(M_{\pi\pi}) \equiv \Gamma_\rho \frac{M_\rho}{M_{\pi\pi}} \left[\frac{M_{\pi\pi}^2 - 4m_\pi^2}{M_\rho^2 - 4m_\pi^2} \right]^{\frac{3}{2}}$$

Minimum bias data

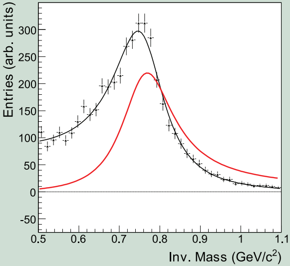

1. Relativistic Breit-Wigner function for ρ peak with amplitude A
2. Constant direct $\pi^+\pi^-$ production amplitude B
3. Söding term for interference of the two
4. 2nd order polynomial f_{BG} describes background from like-sign pairs

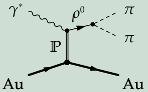

ρ Invariant Mass Fit

PR **C77**, 034910 (2008)

Fit function with 4 components

$$\frac{\mathrm{d}\sigma}{\mathrm{d}M_{\pi\pi}} = \left| A \frac{\sqrt{M_{\pi\pi} M_\rho \Gamma}}{M_{\pi\pi}^2 - M_\rho^2 + i M_\rho \Gamma} + B \right|^2 + f_{\mathrm{BG}}$$

$$\text{with } \Gamma(M_{\pi\pi}) \equiv \Gamma_\rho \frac{M_\rho}{M_{\pi\pi}} \left[\frac{M_{\pi\pi}^2 - 4m_\pi^2}{M_\rho^2 - 4m_\pi^2} \right]^{\frac{3}{2}}$$

1. Relativistic Breit-Wigner function for ρ peak with amplitude A
2. Constant direct $\pi^+\pi^-$ production amplitude B
3. Söding term for interference of the two
4. 2nd order polynomial f_{BG} describes background from like-sign pairs

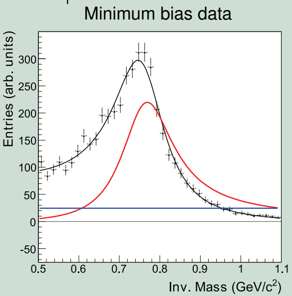

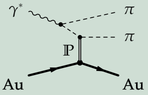

ρ Invariant Mass Fit

PR **C77**, 034910 (2008)

Fit function with 4 components

$$\frac{\mathrm{d}\sigma}{\mathrm{d}M_{\pi\pi}} = \left| A \frac{\sqrt{M_{\pi\pi} M_\rho \Gamma}}{M_{\pi\pi}^2 - M_\rho^2 + i M_\rho \Gamma} + B \right|^2 + f_{\mathrm{BG}}$$

$$\text{with } \Gamma(M_{\pi\pi}) \equiv \Gamma_\rho \frac{M_\rho}{M_{\pi\pi}} \left[\frac{M_{\pi\pi}^2 - 4m_\pi^2}{M_\rho^2 - 4m_\pi^2} \right]^{\frac{3}{2}}$$

1. Relativistic Breit-Wigner function for ρ peak with amplitude A
2. Constant direct $\pi^+\pi^-$ production amplitude B
3. Söding term for interference of the two
4. 2nd order polynomial f_{BG} describes background from like-sign pairs

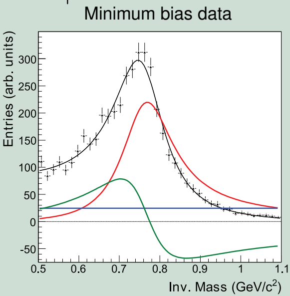

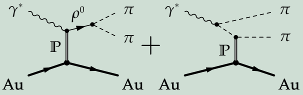

ρ Invariant Mass Fit

PR **C77**, 034910 (2008)

Fit function with 4 components

$$\frac{d\sigma}{dM_{\pi\pi}} = \left| A \frac{\sqrt{M_{\pi\pi} M_\rho \Gamma}}{M_{\pi\pi}^2 - M_\rho^2 + i M_\rho \Gamma} + B \right|^2 + f_{BG}$$

$$\text{with } \Gamma(M_{\pi\pi}) \equiv \Gamma_\rho \frac{M_\rho}{M_{\pi\pi}} \left[\frac{M_{\pi\pi}^2 - 4m_\pi^2}{M_\rho^2 - 4m_\pi^2} \right]^{\frac{3}{2}}$$

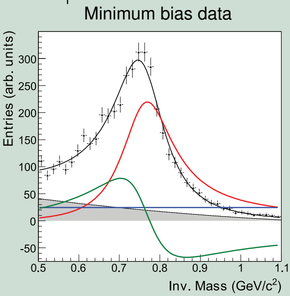

1. Relativistic Breit-Wigner function for ρ peak with amplitude A
2. Constant direct $\pi^+\pi^-$ production amplitude B
3. Söding term for interference of the two
4. 2nd order polynomial f_{BG} describes background from like-sign pairs

Direct $\pi^+\pi^-$ vs. ρ Production

Ratio of non-resonant to resonant $\pi^+\pi^-$ production

$$\frac{d\sigma}{dM_{\pi\pi}} = \left| A \frac{\sqrt{M_{\pi\pi} M_\rho \Gamma}}{M_{\pi\pi}^2 - M_\rho^2 + i M_\rho \Gamma} + B \right|^2 + f_{BG}$$

- Amplitudes A and B are fit parameters
- B/A measure for ratio of non-resonant to resonant $\pi^+\pi^-$ production
  - For Au $\times$ Au @ $\sqrt{s_{NN}} = 200\,\text{GeV}$: $|B/A| = 0.89 \pm 0.08_{\text{stat.}} \pm 0.09_{\text{syst.}}\,\text{GeV}^{-\frac{1}{2}}$
  - No dependence on angles or rapidity

    PR **C77**, 034910 (2008)
  - For Au $\times$ Au @ $\sqrt{s_{NN}} = 130\,\text{GeV}$: $|B/A| = 0.81 \pm 0.08_{\text{stat.}} \pm 0.20_{\text{syst.}}\,\text{GeV}^{-\frac{1}{2}}$

    PRL **89**, 272302 (2002)
  - In agreement with ZEUS EPJ **C2**, 247 (1998)

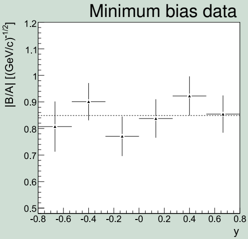

Direct $\pi^+\pi^-$ vs. ρ Production

Ratio of non-resonant to resonant $\pi^+\pi^-$ production

$$\frac{d\sigma}{dM_{\pi\pi}} = \left| A \frac{\sqrt{M_{\pi\pi} M_\rho \Gamma}}{M_{\pi\pi}^2 - M_\rho^2 + i M_\rho \Gamma} + B \right|^2 + f_{BG}$$

- Amplitudes A and B are fit parameters
- B/A measure for ratio of non-resonant to resonant $\pi^+\pi^-$ production
  - For Au $\times$ Au @ $\sqrt{s_{NN}} = 200$ GeV : $|B/A| = 0.89 \pm 0.08_{\text{stat.}} \pm 0.09_{\text{syst.}}\ \text{GeV}^{-\frac{1}{2}}$
  - No dependence on angles or rapidity

    PR **C77**, 034910 (2008)
  - For Au $\times$ Au @ $\sqrt{s_{NN}} = 130$ GeV : $|B/A| = 0.81 \pm 0.08_{\text{stat.}} \pm 0.20_{\text{syst.}}\ \text{GeV}^{-\frac{1}{2}}$

    PRL **89**, 272302 (2002)
  - In agreement with ZEUS EPJ **C2**, 247 (1998)

Minimum bias data

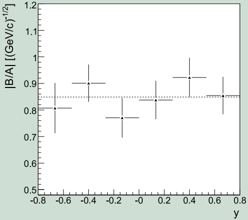

ρ Production Cross Section

Total ρ production cross section for Au $\times$ Au @ $\sqrt{s_{NN}} = 200$ GeV

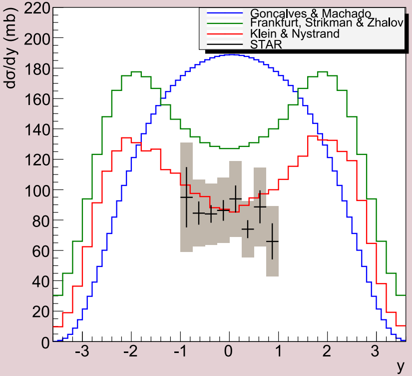

- σ_{tot} obtained by scaling σ_{mb}(nucl. breakup) from minimum bias data with ratio $\dfrac{\sigma_{\text{topo}}(\text{no nucl. breakup})}{\sigma_{\text{topo}}(\text{nucl. breakup})}$ from topology data

ρ Production Cross Section

Coherent and incoherent production

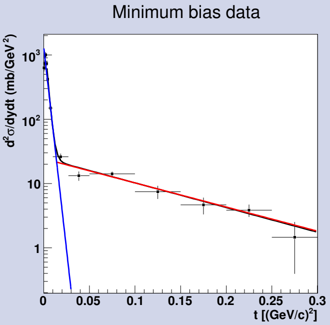

- $t(\approx p_T^2)$-Spectrum fit by double-exponential form
  $$\frac{d\sigma}{dt} = a_{\mathrm{Au}}\, e^{-b_{\mathrm{Au}}\, t} + a_N\, e^{-b_N\, t}$$
- Incoherent production slope
  $b_N = 8.8 \pm 1.0\,\mathrm{GeV}^{-2}$
- Coherent production slope
  $b_{\mathrm{Au}} = 388 \pm 24\,\mathrm{GeV}^{-2}$
  - Related to hadronic radius of gold
- Ratio of incoherent to coherent production
  $$\frac{\sigma_{\mathrm{incoh}}}{\sigma_{\mathrm{coh}}} = 29 \pm 3_{\mathrm{stat.}} \pm 8_{\mathrm{syst.}}\ \%$$

Interference Effects in ρ Photoproduction

PRL **102**, 112301 (2009)

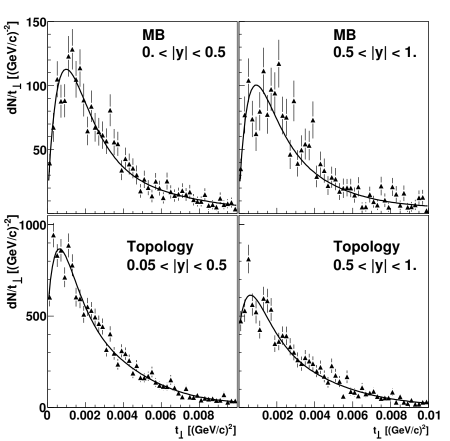

$\tilde{b} \approx 18\,\mathrm{fm}$

$\tilde{b} \approx 46\,\mathrm{fm}$

Weighted average of spectral modification parameter

$$c = 87 \pm 5_{\text{stat.}} \pm 8_{\text{syst.}}\ \%$$

Spin Structure of ρ Production Amplitudes

Extraction of spin density matrix elements from $\pi^+\pi^-$ angular distribution

Schilling, Wolf NP **B61**, 381 (1973)

$$\frac{1}{\sigma}\frac{\mathrm{d}^2\sigma}{\mathrm{d}\cos\theta\,\mathrm{d}\phi} = \frac{3}{4\pi}\left[\frac{1}{2}(1 - r^{04}_{00}) + \frac{1}{2}(3r^{04}_{00} - 1)\cos^2\theta \right.$$
$$\left. - \sqrt{2}\,\mathfrak{Re}[r^{04}_{10}]\,\sin 2\theta\,\cos\phi - r^{04}_{1\,-1}\,\sin^2\theta\,\cos 2\phi\right]$$

- ρ production plane difficult to reconstruct
- Approximate production plane using beam direction
  - θ is polar angle between beam direction and $\vec{p}_{\pi^+}$ in ρ RF
  - ϕ is angle between ρ decay and production plane (w.r.t. beam)
- Due to ambiguity in beam direction cannot measure $\mathfrak{Re}[r^{04}_{10}]$ (interference between helicity non-flip and single-flip)

Spin Structure of ρ Production Amplitudes

Extraction of spin density matrix elements from $\pi^+\pi^-$ angular distribution

$$\frac{1}{\sigma}\,\frac{d^2\sigma}{d\cos\theta\;d\phi} = \frac{3}{4\pi}\left[\frac{1}{2}(1 - r^{04}_{00}) + \frac{1}{2}(3r^{04}_{00} - 1)\cos^2\theta - \sqrt{2}\,\mathfrak{Re}[r^{04}_{10}]\;\sin 2\theta\;\cos\phi - r^{04}_{1\,-1}\;\sin^2\theta\;\cos 2\phi\right]$$

where $\quad r^{04}_{ik} \equiv \dfrac{\rho^0_{ik} + \epsilon R\,\rho^4_{ik}}{1 + \epsilon R}, \quad R = \dfrac{\sigma_L}{\sigma_T}$ Schilling, Wolf NP **B61**, 381 (1973)

- θ is polar angle between beam direction and $\vec{p}_{\pi^+}$ in ρ RF
- ϕ is angle between ρ decay and production plane (w.r.t. beam)
- r^{04}_{00} represents probability that $\lambda_\rho = 0$ for $\lambda_{\gamma^*} = \pm 1$
- $\mathfrak{Re}[r^{04}_{10}]$ related to interference between helicity non-flip and single-flip
- $r^{04}_{1\,-1}$ related to interference between helicity non-flip and double-flip

Spin Structure of ρ Production Amplitudes

Spin density matrix elements from fit of 2D angular distributions

1D projections of 2D angular distribution (minimum bias data)

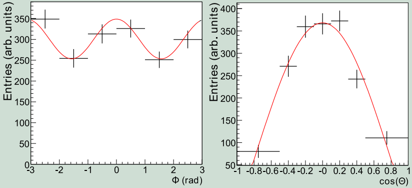

Parameter	STAR	ZEUS
r^{04}_{00}	$-0.03 \pm 0.03_{\text{stat.}} \pm 0.06_{\text{syst.}}$	$0.01 \pm 0.01_{\text{stat.}} \pm 0.02_{\text{syst.}}$
$\Re e[r^{04}_{10}]$	—	$0.01 \pm 0.01_{\text{stat.}} \pm 0.01_{\text{syst.}}$
$r^{04}_{1\,-1}$	$-0.01 \pm 0.03_{\text{stat.}} \pm 0.05_{\text{syst.}}$	$-0.01 \pm 0.01_{\text{stat.}} \pm 0.01_{\text{syst.}}$

- Results similar to ZEUS measurements EPJ **C2**, 247 (1998)
- Spin density elements close to zero indicate s-channel helicity conservation

Spin Structure of ρ Production Amplitudes

Spin density matrix elements from fit of 2D angular distributions

1D projections of 2D angular distribution (minimum bias data)

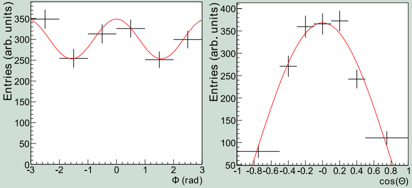

Parameter	STAR	ZEUS
r^{04}_{00}	$-0.03 \pm 0.03_{\text{stat.}} \pm 0.06_{\text{syst.}}$	$0.01 \pm 0.01_{\text{stat.}} \pm 0.02_{\text{syst.}}$
$\mathfrak{Re}[r^{04}_{10}]$	—	$0.01 \pm 0.01_{\text{stat.}} \pm 0.01_{\text{syst.}}$
r^{04}_{1-1}	$-0.01 \pm 0.03_{\text{stat.}} \pm 0.05_{\text{syst.}}$	$-0.01 \pm 0.01_{\text{stat.}} \pm 0.01_{\text{syst.}}$

- Results similar to ZEUS measurements EPJ **C2**, 247 (1998)
- Spin density elements close to zero indicate s-channel helicity conservation

Photonuclear ρ Prod. in d $\times$ Au @ $\sqrt{s_{NN}} = 200\,\text{GeV}$

Asymmetric collision

- γ^* predominantly emitted by Au nucleus
- Topology data
  - Mainly $\gamma^*\,\mathrm{d} \to \rho\,\mathrm{d}$
  - Coherent coupling to entire deuteron
- Topology trigger in coincidence with ZDC neutron signal from deuteron breakup
  - Mainly $\gamma^*\,\mathrm{d} \to \rho\,pn$
  - Coupling to individual nucleons: "incoherent"
- Smaller radii: $R_\mathrm{d} \approx 2\,\mathrm{fm}$, $R_N \approx 0.7\,\mathrm{fm}$ $\Longrightarrow$ ρ has larger p_T

Photonuclear ρ Prod. in d $\times$ Au @ $\sqrt{s_{NN}} = 200\,\text{GeV}$

Asymmetric collision

- γ^* predominantly emitted by Au nucleus
- Topology data
  - Mainly $\gamma^*\,\mathrm{d} \to \rho\,\mathrm{d}$
  - Coherent coupling to entire deuteron
- Topology trigger in coincidence with ZDC neutron signal from deuteron breakup
  - Mainly $\gamma^*\,\mathrm{d} \to \rho\,pn$
  - Coupling to individual nucleons: "incoherent"
- Smaller radii: $R_\mathrm{d} \approx 2\,\mathrm{fm}$, $R_N \approx 0.7\,\mathrm{fm}$ $\Longrightarrow$ ρ has larger p_T

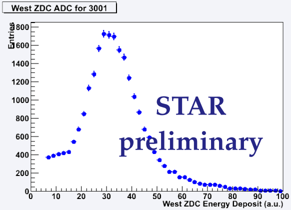

Neutron tagged data

Photonuclear ρ Prod. in d $\times$ Au @ $\sqrt{s_{NN}} = 200\,\text{GeV}$

Asymmetric collision

- γ^* predominantly emitted by Au nucleus
- Topology data
  - Mainly $\gamma^*\,\text{d} \to \rho\,\text{d}$
  - Coherent coupling to entire deuteron
- Topology trigger in coincidence with ZDC neutron signal from deuteron breakup
  - Mainly $\gamma^*\,\text{d} \to \rho\,pn$
  - Coupling to individual nucleons: "incoherent"
- Smaller radii: $R_\text{d} \approx 2\,\text{fm}$, $R_N \approx 0.7\,\text{fm}$
  $\Longrightarrow$ ρ has larger p_T

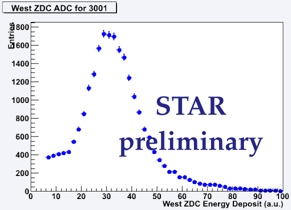

Neutron tagged data

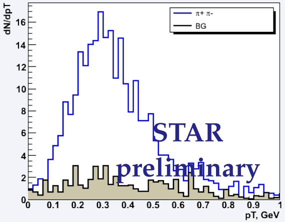

Photonuclear ρ Prod. in d $\times$ Au @ $\sqrt{s_{NN}} = 200\,\text{GeV}$

t-spectrum for d-breakup ("incoherent")

- Exponential fit function: $\mathrm{d}N/\mathrm{d}t = a\,e^{-kt}$
- Slope parameter
  $k = 9.06 \pm 0.85_{\text{stat.}}\ \text{GeV}^{-2}$
  - Related to nucleon form factor
  - Similar to results from
    Au $\times$ Au @ $\sqrt{s_{NN}} = 200\,\text{GeV}$:
    $k = 8.8 \pm 1.0_{\text{stat.}}\ \text{GeV}^{-2}$
    PR **C77**, 034910 (2008)
  - Compatible with ZEUS
    $k = 10.9 \pm 0.3_{\text{stat.}}\ {}^{+1.0}_{-0.5}{}_{\text{syst.}}\ \text{GeV}^{-2}$
    EPJ **C2**, 247 (1998)
- Downturn at low t
  - Not enough energy for d dissociation
  - Also seen in low-energy γd (SLAC 4.3 GeV   Eisenberg *et al.*, NP **B104**, 61 (1976))

Neutron tagged data

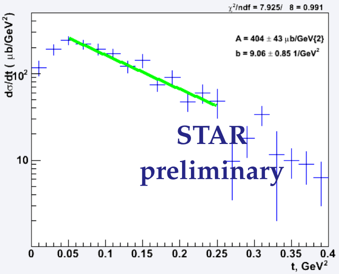

$t \approx t_{\perp} = p_T^2$

Ultra-Peripheral Heavy Ion Collisions (UPC) at STAR

UPC processes measured at STAR (cont.)

3. **Photon-photon interactions with mutual nuclear breakup**
   - e^+e^--pair production in Au $\times$ Au @ $\sqrt{s_{NN}} = 200\,\text{GeV}$

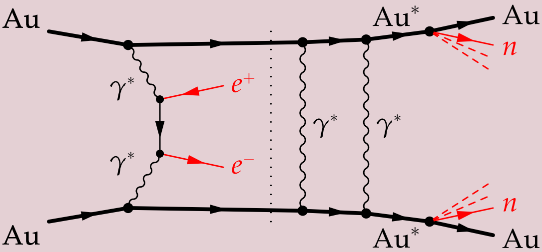

e^+e^--Pair Production in Au $\times$ Au @ $\sqrt{s_{NN}} = 200\,\text{GeV}$

Strong electromagnetic fields

- $Z\alpha \approx 0.6 \implies$ conventional perturbative calculations may be questionable
- Enrich collisions at small impact parameters (= stronger fields) by requiring mutual Coulomb excitation $2R_A < b \lesssim 30\,\text{fm}$

Run 2 minimum bias data

- Challenging measurement due to small acceptance
- Most $e^{\pm}$ produced at very low p_T
  - Reconstructible only at half solenoid field of 0.25 T
- $e^{\pm}$ identification via $\mathrm{d}E/\mathrm{d}x$ in TPC gas
  - Clean sample with PID efficiency close to 1 and minimum contaminations for $p_{e^{\pm}} < 130\,\text{MeV}/c$
- Limited statistics: 52 events

e^+e^--Pair Production in Au $\times$ Au @ $\sqrt{s_{NN}} = 200\,\text{GeV}$

Differential cross sections $d\sigma/dM_{e^+e^-}$ and $d\sigma/dp_T^{e^+e^-}$

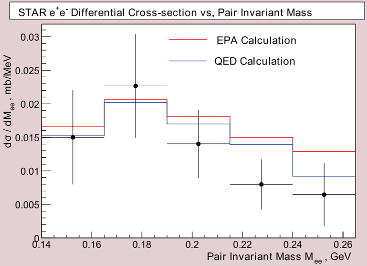

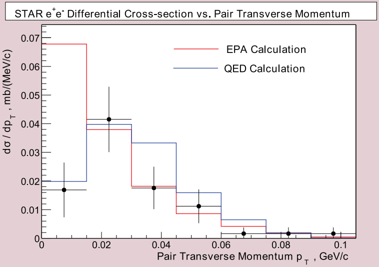

- Data compared with 2 models:
  - **EPA**: equivalent photon approach — PR **C70**, 031902 (2004)
    - Treats γ^* as real photons
    - Fails for lowest p_T bin ($p_T < 15$ MeV/c)
  - **QED**: lowest order QED calculation with simplified model for Coulomb excitation (GDR only) — Henken *et al.*, PR **C69**, 054902 (2004)
    - Describes data well

e^+e^--Pair Production in Au $\times$ Au @ $\sqrt{s_{NN}} = 200\,\text{GeV}$

New QED calculation with realistic phenomenological treatment of Coulomb excitation

Baltz, PRL **100**, 062302 (2008)

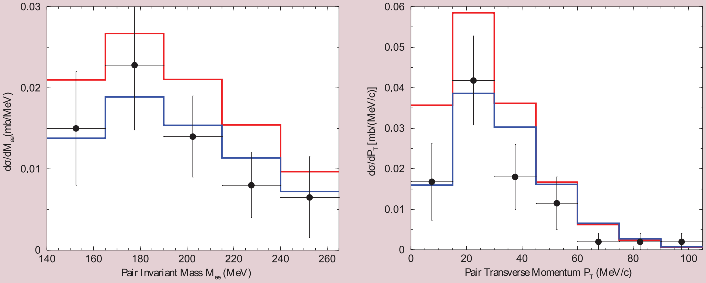

- **Lowest order QED**
  - Overshoots data
    $\sigma_{\text{QED}} = 2.34\,\text{mb}$ vs. $\sigma_{\text{exp}} = 1.6 \pm 0.2_{\text{stat.}} \pm 0.3_{\text{syst.}}\,\text{mb}$
- **Including higher order corrections**
  - Good agreement with data, $\sigma_{\text{QED}} = 1.67\,\text{mb}$

Star Upgrades for 2009+

Time of Flight (ToF) Detector

- Replaces central trigger barrel
- Multi-gap resistive plate chambers (MRPC) using ALICE technology
- 23 000 channels (6 slats $\times$32 plates $\times$120 trays)
- Full coverage of TPC acceptance (2π in ϕ, $|\eta| < 1$)
- Intrinsic time resolution $\approx$ 85 ps

Upgrade of data acquisition (DAQ)

- New TPC front-end electronics based on ALICE's ALTRO chip
- Will permit trigger rates $\mathcal{O}(1\,\mathrm{kHz})$ $\Longrightarrow$ DAQ1000